

Atomic Under-coordination Induced Catalytic and Magnetic Fascinations of Pt and Rh nanoclusters

ShidehAhmadi, Xi Zhang, Yinyan Gong, Chang Q. Sun

Supplementary Information

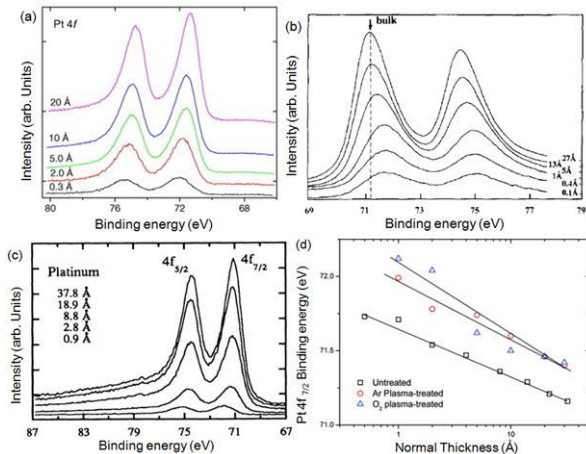
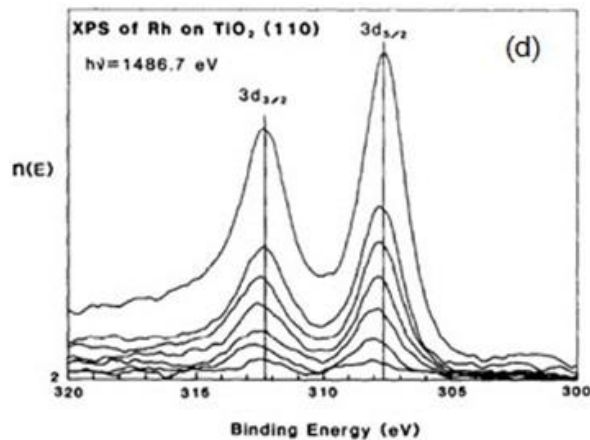
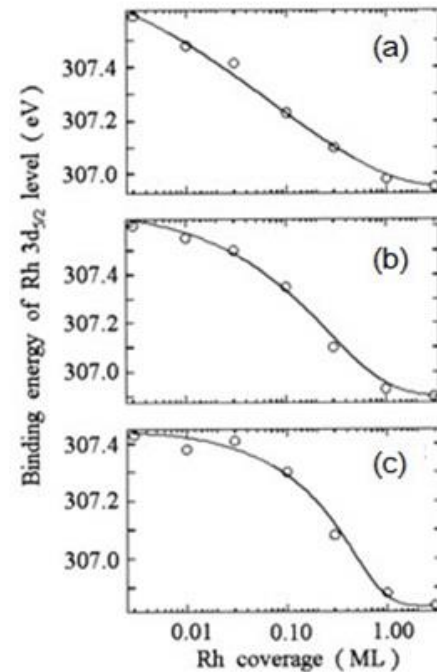


Figure S1. The $4f_{7/2}$ energy shifts positively as the Pt cluster size decreases for Pt deposited on (a) pristine CNTs,¹ (Reprinted with permission from Bittencourt et al., “Platinum–carbon nanotube interaction”, Chem. Phys. Lett. 2008, 462, 260–264. Copyright (2014) by Elsevier), (b) HOPG,² (Reprinted with permission from Marcus et al, “XPS study of the early stages of deposition of Ni, Cu and Pt on HOPG”, Surf. Sci. 1997, 392, 134–142. Copyright (2014) by Elsevier), (c) TiO₂(110) at 300K,³ (Reprinted with permission from Steinruck et al. “Ultrathin films of Pt on TiO₂(110): Growth and chemisorption-induced surfactant effects” Phys. Rev. B. 1995, 51, 2427–2439. Copyright (2014) by the American Physical Society.) and (d) Multi-wall CNT with untreated, and plasma-treated by Ar and O₂,⁴ (Reprinted with permission from Yang et al. “Strongly Enhanced Interaction between Evaporated Pt Nanoparticles and Functionalized Multiwalled Carbon Nanotubes via Plasma Surface Modifications: Effects of Physical and Chemical Defects”, J. Phys. Chem. C 2008, 112, 4075–4082. Copyright (2014) by ACS).



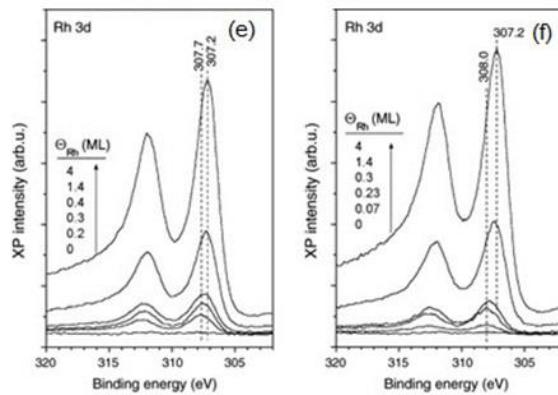


Figure S2. Rh $3d_{5/2}$ energy shifts positively with the decrease of its coverage for Rh deposited on the (a) well-ordered, (b) slightly Ar⁺-pretreated, (c) strongly Ar⁺-pretreated TiO₂(110)-(1x1) surfaces,⁵ (Reprinted with permission from Berkó et. al, “Encapsulation of Rh Nanoparticles Supported on TiO₂(110)-(1 × 1) Surface: XPS and STM Studies”, J. Phys. Chem. B 1998, 102, 3379-3386. Copyright (2014) by ACS), (d) TiO₂ (110) surface at 300K. The spectra corresponds to equivalent Rh coverage of about 0.1, 0.2, 0.3, 0.45, 0.6, 0.75 and 1.5 monolayers (ML).⁶ (Reprinted with permission from Sadeghi and Henrich, “Rh on TiO₂: model catalyst studies of the strong metal-support interaction”. Applications of Surface Science 1984, 19, 330-340. Copyright (2014) by Elsevier), (e) TiO₂ (110) surface at 300 K and (f) TiO₂ (110) surface at 160 K,⁷ (Reprinted with permission from Óvári and Kiss, J., “Growth of Rh nanoclusters on TiO₂: XPS and LEIS studies”. Appl. Surf. Sci. 2006, 252, 8624-8629. Copyright (2014) by Elsevier).

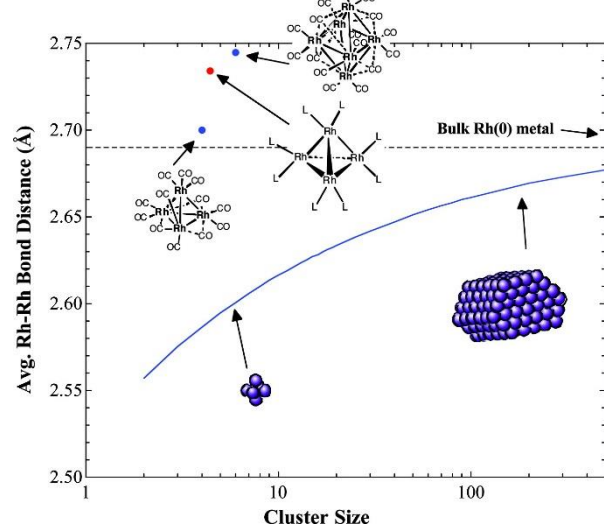
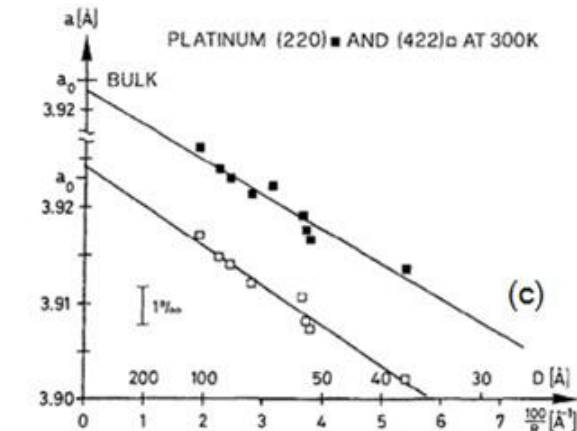
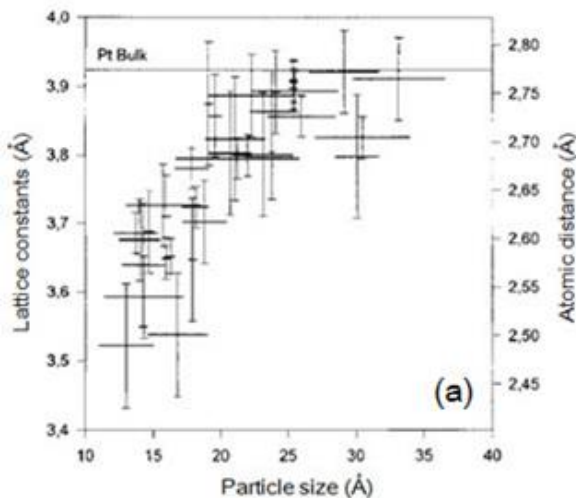
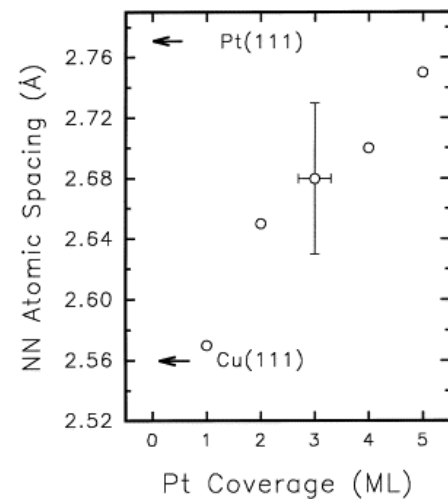
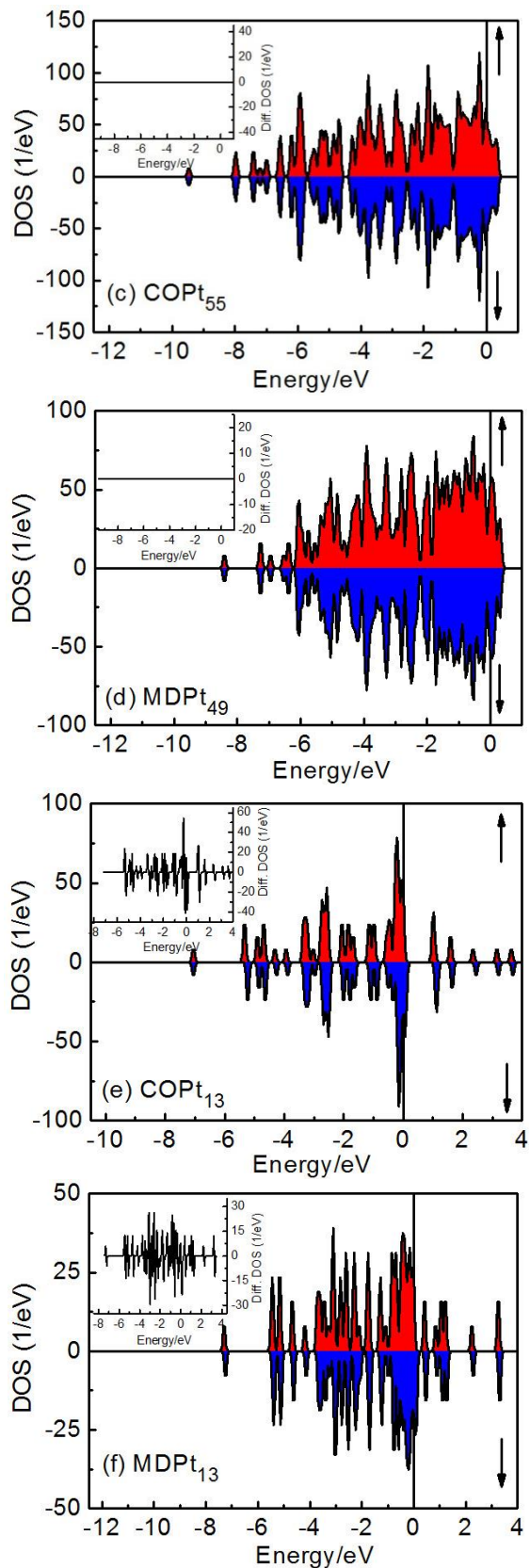
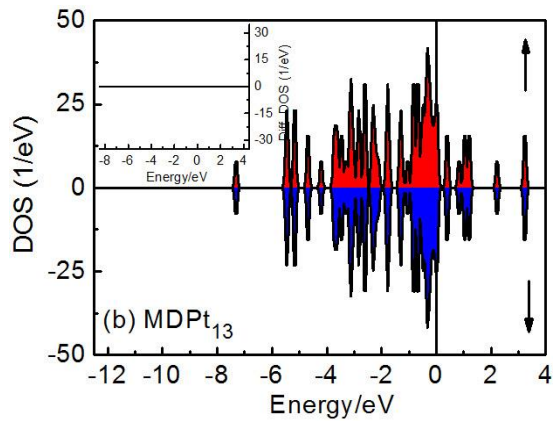
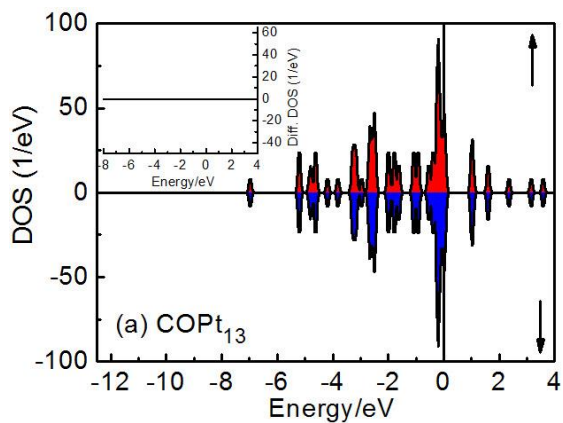


Figure S3. Lattice constant contracts with reducing the nanoparticle size for Pt deposited on (a) NiAl(110) substrate,⁸ (Reprinted with permission from Klimenkov et.al, “The structure of Pt-aggregates on a supported thin

aluminum oxide film in comparison with unsupported alumina: a transmission electron microscopy study”, Surf. Sci. 1997, 391, 27-36. Copyright (2014) by Elsevier), (b) Cu (111) at 300K,⁹ (Reprinted with permission from Shen et. al, “Stacking and structure of platinum on Cu (1 1 1) up to five monolayers”, Nuclear Instruments and Methods in Physics Research Section B: Beam Interactions with Materials and Atoms 1998, 335, 361-365. Copyright (2014) by Elsevier), (c) Pt (422) and Pt (111) at 300K,¹⁰ (Reprinted with permission from Solliard and Flueli, “Surface stress and size effect on the lattice parameter in small particles of gold and platinum”, Surf. Sci. 1985, 156, Part 1, 487-494. Copyright (2014) by Elsevier), and (d) Rh,¹¹ (Reprinted with permission from Fulton et. al, “When is a Nanoparticle a Cluster? An Operando EXAFS Study of Amine Borane Dehydrocoupling by Rh4-6 Clusters”, J. Am. Chem. Soc. 2007, 129, 11936-11949. Copyright (2014) by ACS).



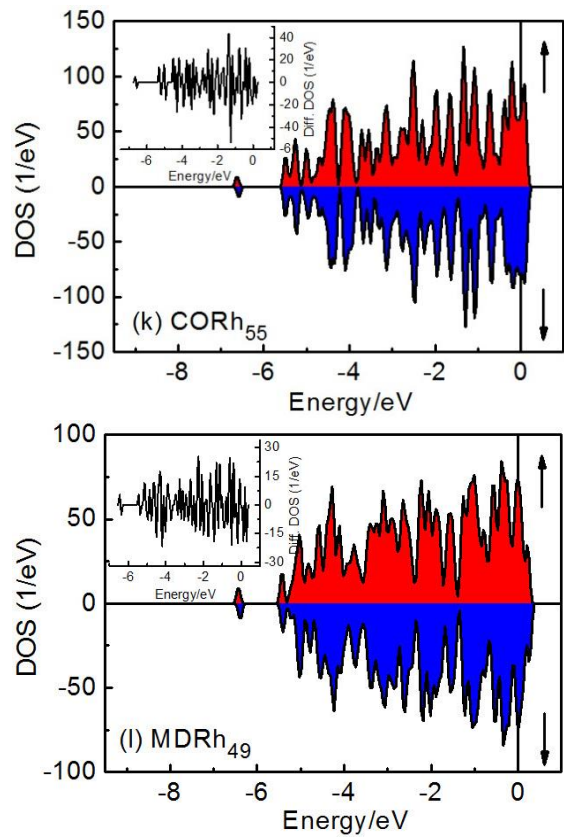
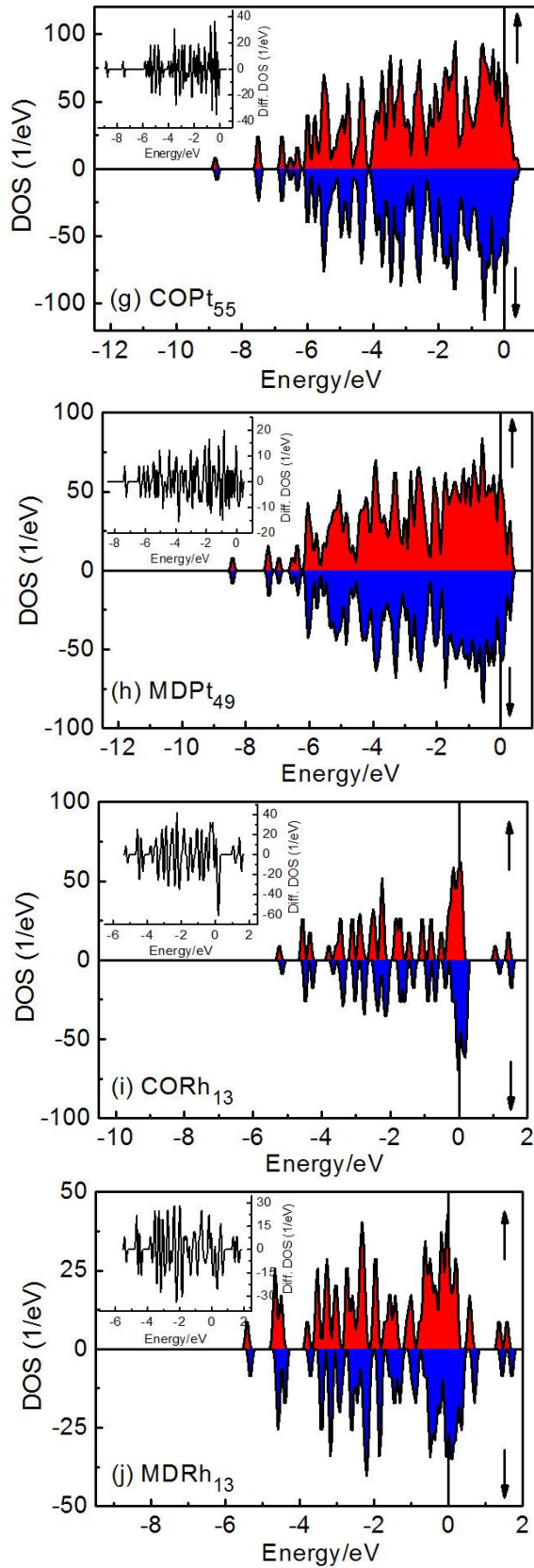
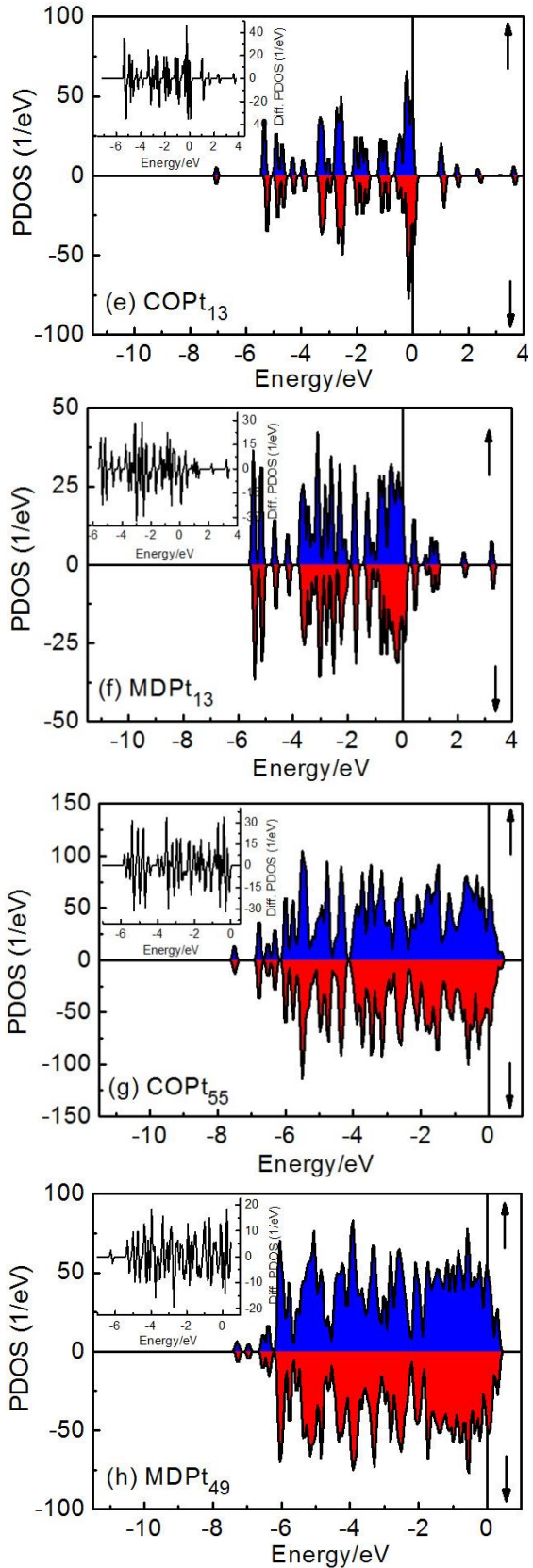
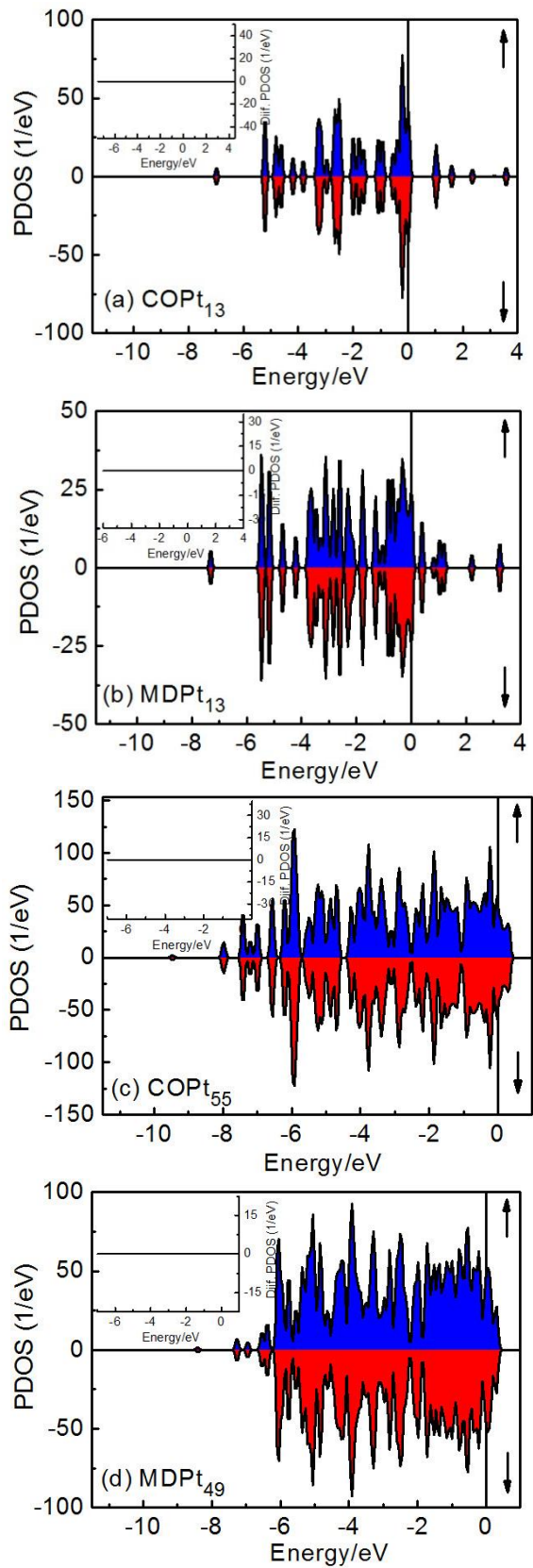


Figure S4. The spin-polarized DOS of (a-d) 5d-Pt singlet state, and (e-h) 5d-Pt triplet state, and (i-l) 4d-Rh quartet state. Inset is the difference between spin-up and spin-down states in DOS. The spin-up and spin-down configurations are indicated by the up and down arrows, respectively. The Fermi level is set at 0 eV. Same as CO_{147} and MD_{75} of Pt and Rh NPs shown in Figure 6 of the main text, the DOS distributions of spin-up and spin down states split for triplet state of Pt and quartet state of Rh whereas no split for the singlet state of Pt for various cluster sizes and structures, indicating the magnetic property is related to the under-coordinated atoms in the skin regardless of the size and structures of Pt and Rh NPs.



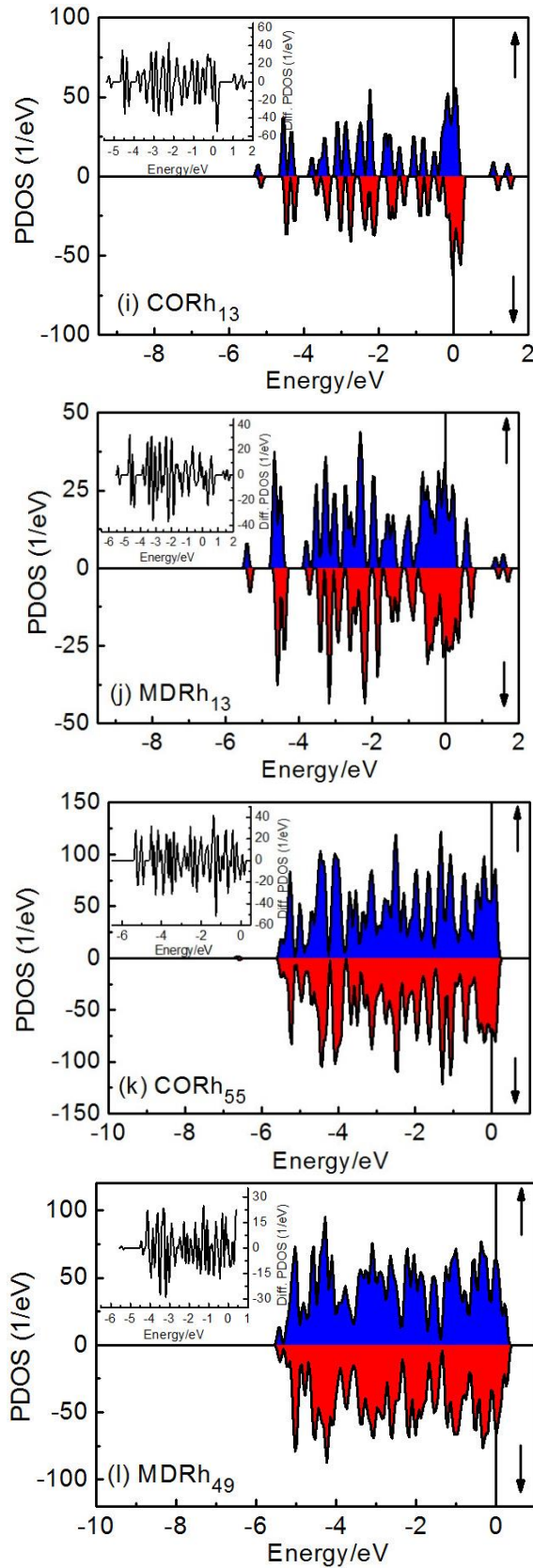


Figure S5. The spin-polarized PDOS of (a-d) 5d-Pt singlet state, (e-h) 5d-Pt triplet state, and (i-l) 4d-Rh quartet state. Inset is the difference between spin-up and spin-down states in DOS. The spin-up and spin-down configurations are indicated by the up and down arrows, respectively. The Fermi level is set at 0 eV. Same as CO₁₄₇ and MD₇₅ of Pt and Rh NPs shown in Figure 6 of the main text, the PDOS distributions of spin-up and spin down states split for triplet state of Pt and quartet state of Rh whereas no split for the singlet state of Pt for various cluster sizes and structures, indicating the magnetic property is related to the under-coordinated atoms in the skin regardless of the size and structures of Pt and Rh NPs.

Table S1. The effective CN (z_i), bond length (d_i),¹²⁻²¹ bond contraction coefficient (C_i), shell index (i), magnetic moment (μ),²²⁻²⁶ and “charge transfer” of atoms²⁷⁻³¹ at different positions of Pt_{13} and Rh_{13} nanoclusters. The results obtained by double numerical (DN) basic set in Dmol³.³²

Structure	Position atom	z_i	d_i (Å)		C_{i-1} (%)		Shell i	Magnetic moment (μ)		“Charge Transfer” (e)		
			Pt Singlet	Pt Triplet	Rh	Pt Singlet		Pt Triplet	Rh	Pt Singlet	Pt Triplet	Rh
CO_{13}	1~2	2.00	2.716	2.716	2.652	-2.14	-2.12	-1.39	1	1.896	2.856	-0.120
	MD ₁₃	2~4	-	2.696	2.696	2.625	-2.84	-2.84	-	-	-	-0.120
	1~3	2.43	2.793	2.793	2.715	-28.83	-28.83	-28.64	1	1.894	2.850	-0.087

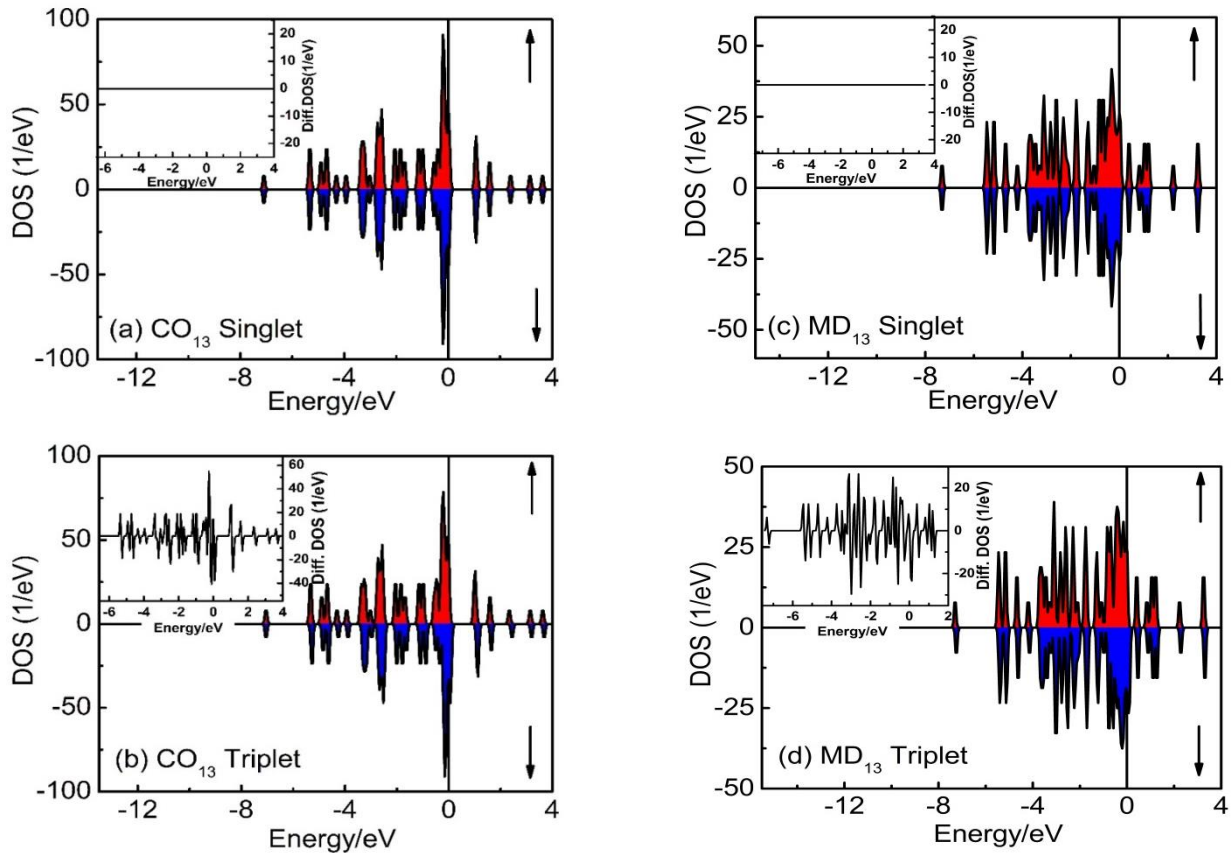


Figure S6. The spin-polarized DOS of Pt with singlet and triplet states for (a-b) CO_{13} and (c-d) MD_{13} structures calculated by DN basic set in Dmol³. Inset is the difference between spin-up and spin-down states in DOS. The spin-up and spin-down configurations are indicated by the up and down arrows, respectively. The Fermi level is set at 0 eV.

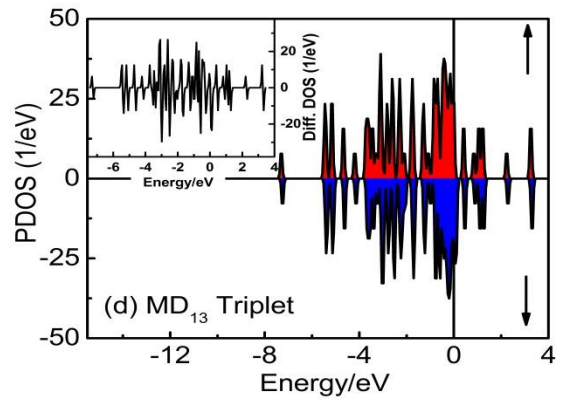
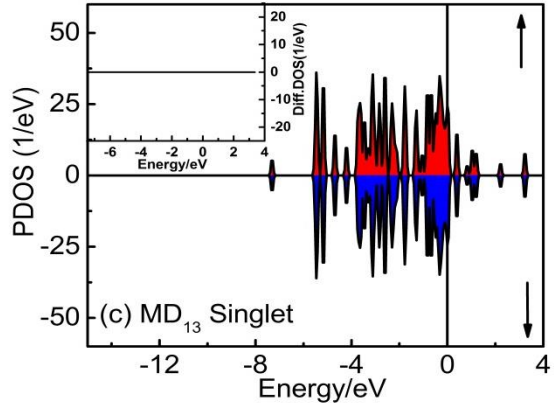
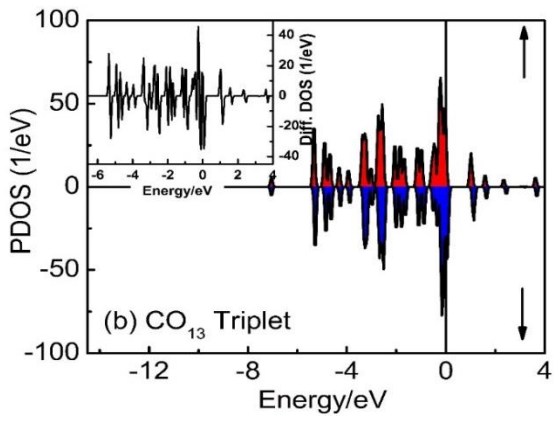
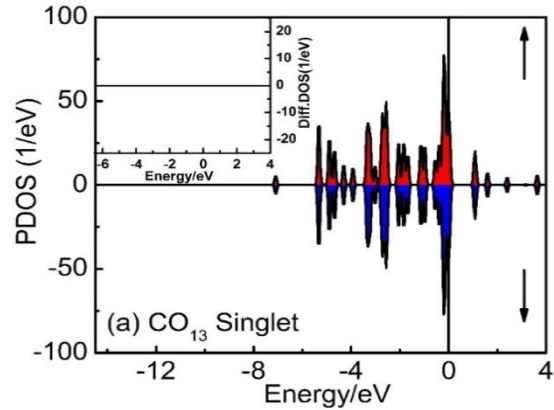


Figure S7. The spin-polarized PDOS of Pt with singlet and triplet states (a-b) CO₁₃ and (c-d) MD₁₃ structures calculated by DN basic set in Dmol³. Inset is the difference between spin-up and spin-down states in PDOS. The spin-up and spin-down configurations are indicated by the up and down arrows, respectively. The Fermi level is set at 0 eV.

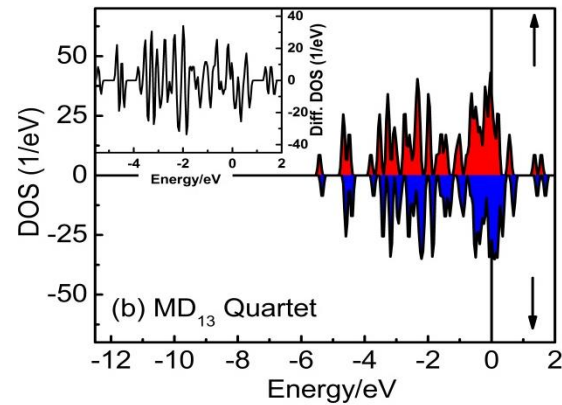
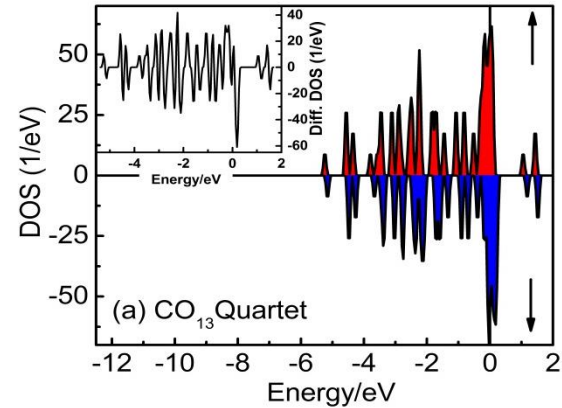


Figure S8. The spin-polarized DOS of Rh with quartet state (a) CO₁₃ and (b) MD₁₃ structures calculated by DN basic set in Dmol³. Inset is the difference between spin-up and spin-down states in DOS. The spin-up and spin-down

configurations are indicated by the up and down arrows, respectively. The Fermi level is set at 0 eV.

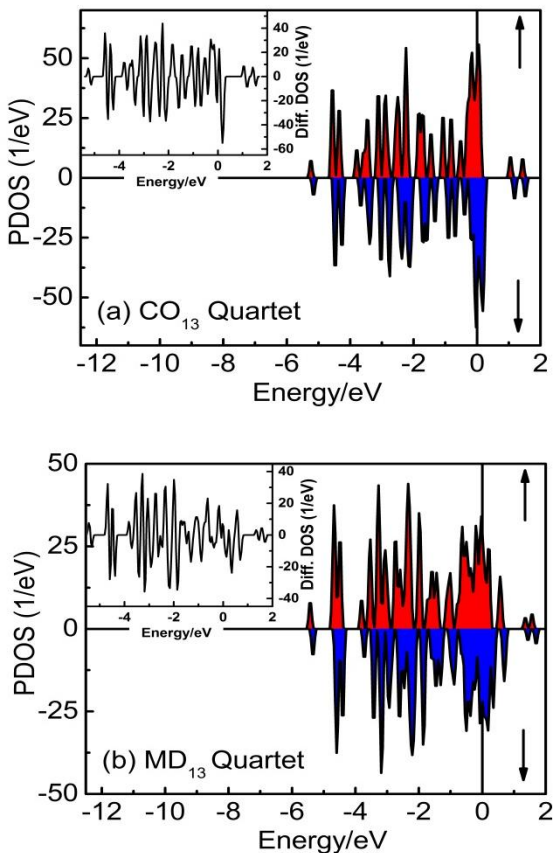


Figure S9. The spin-polarized PDOS of Rh with quartet state (a) CO_{13} and (b) MD_{13} structures calculated by DN basic set in Dmol³. Inset is the difference between spin-up and spin-down states in PDOS. The spin-up and spin-down configurations are indicated by the up and down arrows, respectively. The Fermi level is set at 0 eV.

REFERENCES

1. C. Bittencourt, M. Hecq, A. Felten, J. J. Pireaux, J. Ghijssen, M. P. Felicissimo, P. Rudolf, W. Drube, X. Ke and G. Van Tendeloo, *Chem. Phys. Lett.*, 2008, **462**, 260-264.
2. P. Marcus and C. Hinnen, *Surf. Sci.*, 1997, **392**, 134-142.
3. H.-P. Steinrück, F. Pesty, L. Zhang and T. E. Madey, *Phys. Rev. B*, 1995, **51**, 2427-2439.
4. D.-Q. Yang and E. Sacher, *J. Phys. Chem. C*, 2008, **112**, 4075-4082.
5. A. Berkó, I. Ulrych and K. C. Prince, *J. Phys. Chem. B*, 1998, **102**, 3379-3386.
6. H. R. Sadeghi and V. E. Henrich, *Appl. Surf. Sci.*, 1984, **19**, 330-340.
7. L. Óvári and J. Kiss, *Appl. Surf. Sci.*, 2006, **252**, 8624-8629.
8. M. Klimentov, S. Nepijko, H. Kuhlenbeck, M. Bäumer, R. Schlägl and H. J. Freund, *Surf. Sci.*, 1997, **391**, 27-36.
9. Y. G. Shen, D. J. O'Connor and R. J. MacDonald, *Nuclear Instruments and Methods in Physics Research Section B: Beam Interactions with Materials and Atoms*, 1998, **135**, 361-365.
10. C. Sollaard and M. Flueli, *Surf. Sci.*, 1985, **156**, Part 1, 487-494.
11. J. L. Fulton, J. C. Linehan, T. Autrey, M. Balasubramanian, Y. Chen and N. K. Szymczak, *J. Am. Chem. Soc.*, 2007, **129**, 11936-11949.
12. X. Liu, M. Bauer, H. Bertagnolli, E. Roduner, J. van Slageren and F. Philipp, *Phys. Rev. Lett.*, 2006, **97**, 253401-253404.
13. S. R. Bahri and K. W. Jacobsen, *Phys. Rev. Lett.*, 2001, **87**, 266101-266104.
14. R. H. M. Smit, C. Untiedt, A. I. Yanson and J. M. van Ruitenbeek, *Phys. Rev. Lett.*, 2001, **87**, 266102-266105.
15. J. Bartolomé, F. Bartolomé, L. M. García, E. Roduner, Y. Akdogan, F. Wilhelm and A. Rogalev, *Phys. Rev. B*, 2009, **80**, 014404-014413.
16. H. Y. Sang, A. D. David, B. A. James, O. Pablo and G. Keith, *J. Phys.: Condens. Matter*, 1997, **9**, L39-L45.
17. K. Balasubramanian, *J. Chem. Phys.*, 1987, **87**, 6573-6578.
18. L. Zhi-Qiang, Y. Jing-Zhi, K. Ohno and Y. Kawazoe, *J. Phys.: Condens. Matter*, 1995, **7**, 47-53.
19. Y. Jinlong, F. Toigo and W. Kelin, *Phys. Rev. B*, 1994, **50**, 7915-7924.
20. P. Villaseñor-González, J. Dorantes-Dávila, H. Dreyssé and G. M. Pastor, *Phys. Rev. B*, 1997, **55**, 15084-15091.
21. C. Barreteau, M. C. Desjonquères and D. Spanjaard, *Eur. Phys. J. D*, 2000, **11**, 395-402.
22. D. Sellmyer and S. Ralph, *Advanced magnetic nanostructures*, Springer, New York, 2006.
23. H. Sun, Y. Ren, Y.-H. Luo and G. Wang, *Physica B: Condens. Matter*, 2001, **293**, 260-267.
24. E. O. Berlanga-Ramírez, F. Aguilera-Granja, A. Díaz-Ortíz, J. L. Rodríguez-López and A. Vega, *Phys. Lett. A*, 2003, **318**, 473-479.
25. F. Aguilera-Granja, J. M. Montejano-Carrizales and J. L. Morán-López, *Phys. Lett. A*, 1998, **242**, 255-260.
26. P. J. Jensen and K. H. Bennemann, *Z. Phys. D*, 1995, **35**, 273-278.
27. R. L. J. Fuyi Chen, *Acta Mater.*, 2008, **56**, 2374-2380.
28. X. Zhang, J.-I. Kuo, M. Gu, X. Fan, P. Bai, Q.-G. Song and C. Q. Sun, *Nanoscale*, 2010, **2**, 412-417.
29. C. J. Heard and R. L. Johnston, *Eur. Phys. J. D*, 2013, **67**, 1-6.
30. A. Moghaddasi, M. Zahedi and P. Watson, *J. Phys. Chem. C*, 2012, **116**, 5014-5018.

31. S. Ahmadi, X. Zhang, Y. Gong, C. H. Chia and C. Q. Sun, *Phys. Chem. Chem. Phys.*, 2014, **16**, 8940-8948.
32. B. Delley, *J. Chem. Phys.*, 1990, **92**, 508-517.